

Kinetic energy offsets for multicharged ions from an electron beam ion source

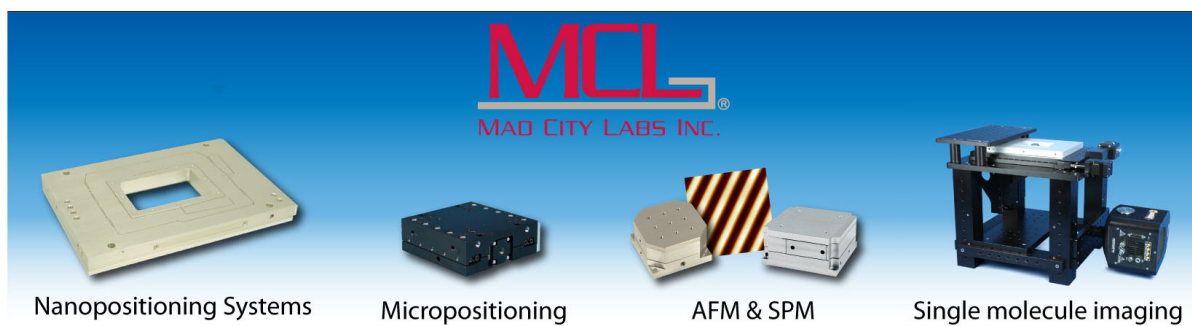
D. D. Kulkarni, C. D. Ahl, A. M. Shore, A. J. Miller, J. E. Harriss, C. E. Sosolik, and J. P. Marler

Citation: [Review of Scientific Instruments](#) **88**, 083306 (2017); doi: 10.1063/1.4997962

View online: <http://dx.doi.org/10.1063/1.4997962>

View Table of Contents: <http://aip.scitation.org/toc/rsi/88/8>

Published by the [American Institute of Physics](#)



Kinetic energy offsets for multicharged ions from an electron beam ion source

D. D. Kulkarni, C. D. Ahl, A. M. Shore, A. J. Miller, J. E. Harriss, C. E. Sosolik, and J. P. Marler
Department of Physics and Astronomy, Clemson University, Clemson, South Carolina 29634, USA

(Received 14 January 2017; accepted 26 July 2017; published online 21 August 2017)

Using a retarding field analyzer, we have measured offsets between the nominal and measured kinetic energy of multicharged ions extracted from an electron beam ion source (EBIS). By varying source parameters, a shift in ion kinetic energy was attributed to the trapping potential produced by the space charge of the electron beam within the EBIS. The space charge of the electron beam depends on its charge density, which in turn depends on the amount of negative charge (electron beam current) and its velocity (electron beam energy). The electron beam current and electron beam energy were both varied to obtain electron beams of varying space charge and these were related to the observed kinetic energy offsets for Ar^{4+} and Ar^{8+} ion beams. Knowledge of these offsets is important for studies that seek to utilize slow, i.e., low kinetic energy, multicharged ions to exploit their high potential energies for processes such as surface modification. In addition, we show that these offsets can be utilized to estimate the effective radius of the electron beam inside the trap. *Published by AIP Publishing.* [<http://dx.doi.org/10.1063/1.4997962>]

I. INTRODUCTION

Multicharged ions or MCIs are of interest in multiple contexts due to the high potential energies they possess relative to those typically encountered with singly charged ions.¹ This potential energy component leads to large charge-exchange cross sections for MCIs when they encounter a target atom or molecule. In the case of solid targets, this charge exchange can couple into irreversible changes in the structure and many have proposed MCIs as a route to single-atom nanostructuring at surfaces.^{2–4} However, in order to exploit this potential energy effectively, the interaction time between the MCI and the target must be maximized, which implies a need for ions with low kinetic energies. The unique methods by which MCIs are produced, such as in an electron beam ion trap (EBIT) or source (EBIS), can lead to large (>100 eV) offsets in the extracted energies for such ions.^{5,6} In this article, we focus on measuring these offsets for MCIs produced in an EBIS device.

Electron beam ion sources produce MCIs by confining and repetitively ionizing a source material using a combination of drift tubes and a coaxial electron beam^{7,8} (see Fig. 1). The drift tubes within an EBIS provide an axial trapping potential, while the electron beam serves to both ionize the beam source material through electron impact ionization and trap the generated ions radially through a “space charge” effect. The space charge potential produced by the electron beam is dependent on its current and kinetic energy. In general, more negative charge (higher electron beam current I_e) will increase the trapping potential, while a lower linear charge density (higher velocity v_e or equivalently higher electron beam energy E_e) will lower the trapping potential. In other words, the charge density of the electron beam is proportional to (I_e/v_e) , leading to an inverse square root dependence on energy and a linear dependence on the current. These changes in the trap potential related to the space charge will lead to

offsets in the kinetic energy of any extracted ions. Therefore, calibrating an EBIS for space charge effects is important if one seeks to produce well-defined MCI beams with low kinetic energy.

In this paper, we utilize retarding field measurements, coupled with a systematic variation in the electron beam parameters to characterize EBIS-produced beams of MCIs. In Sec. II, we present the details of our experimental apparatus, including the EBIS, its attached beamline and deceleration optics, and our retarding field analyzer (RFA). In Sec. III, we discuss the results of our kinetic energy offset measurements for argon MCIs and how they relate to trapping conditions within the EBIS (electron beam current and electron kinetic energy). Our results are summarized in Sec. IV.

II. EXPERIMENT

Our measurements were conducted on the EBIS-SC at the Clemson University Electron Beam Ion Trap (CUEBIT) facility described in detail in Ref. 9. As noted in Sec. I, the EBIS produces MCIs by interacting a neutral gas target with a high current (few 100 mA), high energy electron beam (maximum 20 keV). The electrons are compressed in the trap center by a strong magnetic field gradient. By tuning the electron beam characteristics and the trapping time, one can optimize the source to produce a desired MCI charge state distribution. The generated MCIs are trapped axially by the electrostatic potentials (U_L , U_C , and U_R) applied to the three sections of the drift tube (DT_L , DT_C , and DT_R) as illustrated in Fig. 1. Radial trapping of MCIs is provided by the strong negative potential of the coaxial electron beam passing through the drift tube. The potential applied to the rightmost drift tube section (DT_R) is used to control the manner in which ions are released from the drift tube into the beamline. If U_R is dropped quickly below U_C , then the MCIs are released in a pulse. If U_R is maintained slightly higher than U_C , then some MCIs escape continuously

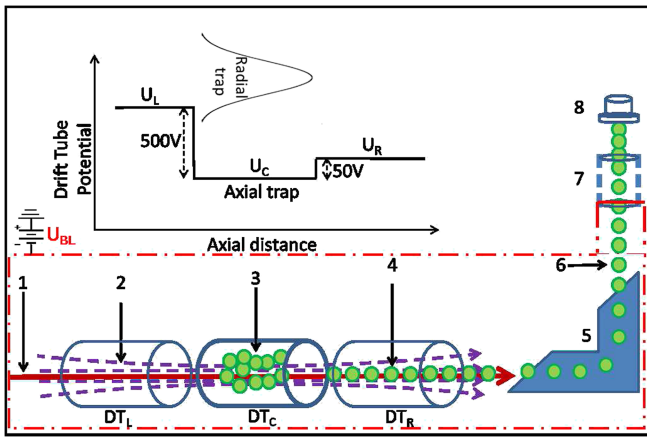


FIG. 1. A schematic of the experimental setup for the EBIS, beamline, and RFA (1—electron beam, 2—magnetic field (6 T), 3—trapped ion cloud, 4—extracted ion beam, 5—analyzing magnet, 6—charge-to-mass ratio separated ion beam, 7—deceleration lens, and 8—RFA). The potential profile for ions trapped within the EBIS is illustrated above the drift tube (DT) sections along with typical applied electrostatic potentials (U), with subscripts signifying position: L—leftmost, C—central, and R—rightmost. The central drift tube section (DT_C) is highlighted as it is the ion trapping region. The ions are trapped axially in section DT_C due to the potential well created as shown, while the space charge of the electron beam produces a trapping potential in the radial direction. U_{BL} is set as negative for decelerated beams and positive for accelerated beams of positive ions.

(“leaky” mode).^{10–13} For these measurements, the EBIS was operated in leaky mode with U_R set to 50 V above U_C . This value was chosen as an optimal value for extracted ion flux for the chosen charge states.

Within the EBIS, the electron beam is continuously dumped to a collector plate, while the MCIs extracted from DT_R are guided down a connected UHV beamline and accelerated to an energy of $(Q \times U_R)$ eV to form an ion beam, where Q is the charge state of the ions. To separate out ions with a particular charge state Q , this ion beam, consisting of a distribution of masses and charge states, is passed through an analyzing or bending magnet that selectively passes ions based on their charge-to-mass ratio. The beamline is held at a pressure of $\sim 10^{-9}$ Torr to minimize recombination, while it is floated to a negative potential (U_{BL}) to facilitate deceleration. A six-element deceleration lens connected to the end of the beamline both slows down the beam and focuses it within a zone 25 mm to 50 mm beyond the end of the lens. The ions are decelerated to a final kinetic energy of $[Q \times (U_R - |U_{BL}|)]$ eV.

For this study, a retarding field analyzer (RFA), shown schematically in Fig. 2, was placed within the range of the focal length of the deceleration lens. The RFA position was held constant for all the measurements reported here. The ion current was optimized for each beam setting by appropriately focusing the ion beam using the energy-conserving elements of the deceleration lens. The purpose of the RFA was to measure the kinetic energy of the extracted MCI beams.

The RFA consists of the following electrically isolated components: a faceplate (FP) used for alignment, a hollow cylindrical main body (MB), a retarding plate (RP), and a Faraday cup (FC) detector. The aperture sizes of the FP and RP were 3 mm and 4 mm, respectively. The MB here serves only as a spacer, though it is designed as the body of a gas

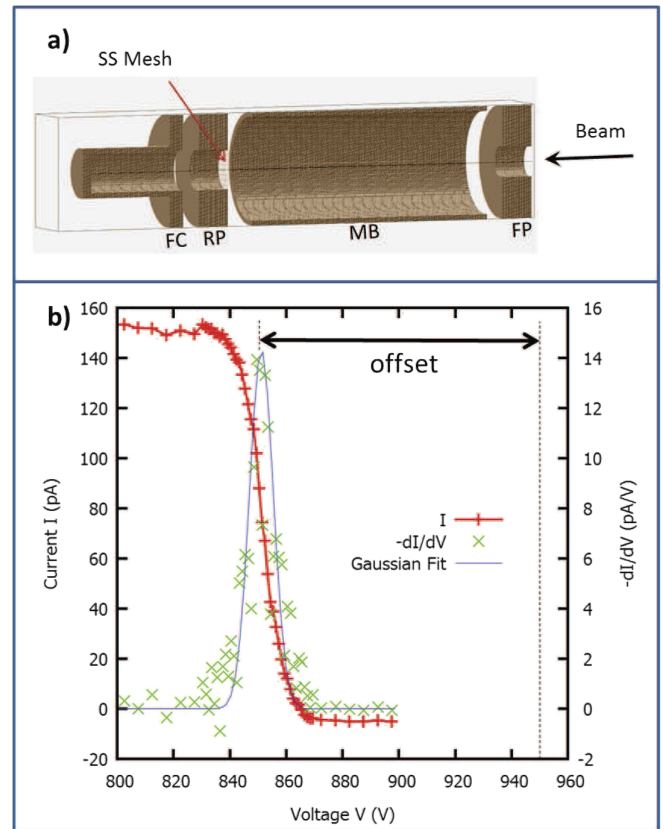


FIG. 2. (a) A model of the RFA using SIMION¹⁴ showing the internal components of the RFA—the faceplate (FP), the main body (MB), the retarding plate (RP) with SS mesh, and the Faraday Cup (FC) detector. (b) An example RFA curve for an Ar^{8+} beam (+) and the computed derivative (x) fit to a Gaussian. As seen in the figure, the kinetic energy of the ion beam as measured by the RFA (851.3 eV/Q) is offset from the nominal kinetic energy calculated from the trap potentials (950 eV/Q) by 98.7 eV/Q.

cell for future experiments to study MCI charge exchange in gases. The RP was electrically connected to a high-voltage MHV feedthrough, allowing the application of potentials up to 5 kV. To avoid a sag in the potential due to the RP aperture, a grid (SS type 316, mesh 20, wire diameter 0.004”) was spot welded to the RP. The maximum expected value for the potential sag with this mesh was calculated to be 0.2% [see Eq. (1) in Ref. 15]. For all measurements, the nominal kinetic energy of the ion beam was set at 950 eV/Q by appropriately adjusting the trap and beamline voltages. Simulations performed using SIMION showed that the minimum energy required by these ions to pass through the RP was 2 eV/Q lower than the voltage applied to the RP-mesh.

The procedure for measuring the kinetic energy of a given MCI beam involved varying the potential applied to the RP while monitoring the beam current in the FC detector. All extracted MCI beams arrived at the RFA as continuous, i.e., non-pulsed, beams and the current collected in the FC detector was measured by a Keithley 6485 picoammeter interfaced to a digital computer for data acquisition. A significant difference was observed between the kinetic energies of the extracted MCI beams measured with the RFA and the nominal kinetic energies based on the drift tube potential settings of the EBIS. To determine the relationship between this offset in kinetic energy and the negative space charge of the electron beam in

the ion source, both the current and the energy of the electron beam were varied while extracting Ar^{Q+} ($Q = 4, 8$) ion beams with a nominal energy of $950 \text{ eV}/Q$. Specifically, the electron beam current (I_e) from the cathode emitter was varied from 60 mA to 220 mA in steps of 40 mA at a fixed cathode potential ($U_{\text{cath}} = -600 \text{ V}$), and the electron beam energy (E_{e0}) was varied from 3.6 keV to 6.6 keV in steps of 1 keV. The electron energy E_{e0} is determined from the sum of the cathode potential U_{cath} and the potential on the central drift tube U_C and is given by $E_{e0} = |e| \times (U_C + |U_{\text{cath}}|)$, where e is the charge of an electron.

III. RESULTS AND DISCUSSION

For an MCI beam of charge state Q extracted in leaky mode from the EBIS, the expected kinetic energy (E_0), excluding effects of the space charge potential, is given by the following:

$$E_0/Q = U_R - |U_{\text{BL}}|. \quad (1)$$

For any ion beam, the space charge effect will reduce the kinetic energy by an amount, U_{sp} , as shown here,

$$E/Q = E_0/Q - |U_{\text{sp}}|. \quad (2)$$

For the ion beams extracted from the EBIS in this study, the drift tube and beamline voltages were varied appropriately to generate ions with nominal kinetic energies of $950 \text{ eV}/Q$. Subsequent measurements within the RFA of the actual kinetic energy showed shifts from these expected values, which we hereafter refer to as the kinetic energy offset ΔE . Measured kinetic energy offsets for beams of Ar^{4+} are shown in Fig. 3 as a function of the electron beam current I_e within the EBIS for four different values of the electron beam energy E_{e0} . From these data, one can see that there is a linear dependence of ΔE on the electron beam current for all electron beam energies. A similar linear dependence was measured for Ar^{8+} ions as well. At individual values of the electron beam current, it is also clear that the offsets vary inversely with the electron beam energy. Similar data for Ar^{8+} ions are shown in Fig. 4, now as a function of the electron beam energy. Here a log-log plot is used to highlight the inverse dependence on electron beam energy and the fitted lines shown all have a slope of ~ -0.5 . Similar data analysis of measurements with the Ar^{4+} ions also yielded slopes of ~ -0.5 . This slope signifies the inverse dependence on the square root of the energy of the electron beam, i.e., the velocity of the electron beam as mentioned earlier.

To understand the dependence of ΔE on I_e and E_{e0} observed in Figs. 3 and 4, we note that the space charge potential can be estimated as¹⁶

$$U_{\text{sp}} \approx \frac{I_e}{4\pi\epsilon_0 v_e} \left(2 \ln \left[\frac{r_{\text{drift tube}}}{r_{\text{electron beam}}} \right] + 1 \right), \quad (3)$$

where $v_e = \sqrt{2E_{e0}/m_e}$ is the velocity of the electron beam and $r_{\text{drift tube}}$ and $r_{\text{electron beam}}$ refer to the radii of the EBIS drift tube and the electron beam, respectively. If one assumes that the effective electron beam radius in DT_C remains constant for the different beams across all source settings, the primary parameters which determine the magnitude of U_{sp} are the

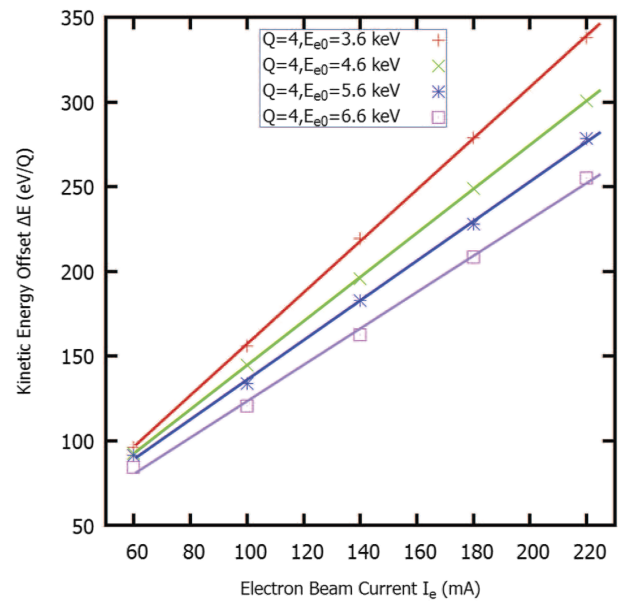


FIG. 3. Offset in the kinetic energy of the MCI beam measured at the RFA from the expected value as a function of the electron beam current (I_e) at different values of nominal electron beam energy (E_{e0}) for Ar^{4+} .

electron beam current and velocity. The linear dependence on I_e is clearly demonstrated in the data of Fig. 3, while the inverse dependence on the velocity is present in Fig. 4.

The qualitative agreement illustrated in Figs. 3 and 4 between our measured kinetic energy offsets and the functional dependencies of the space charge on I_e and E_{e0} [Eq. (3)] suggests that the space charge potential of the electron beam within the EBIS is the source of these offsets. Knowing that, it becomes important to find a quantitative relationship for a given EBIS source that can be utilized for predicting and accounting for these offsets in any experimental design.

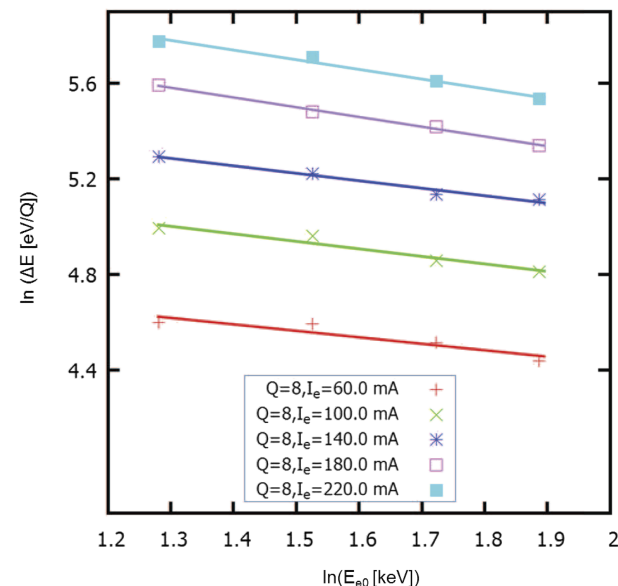


FIG. 4. A log-log plot of the offset in the kinetic energy of the MCI beam (in eV/Q) measured at the RFA from the expected value as a function of the nominal electron beam energy (E_{e0}) (in keV) at different values of electron beam current (I_e) for Ar^{8+} .

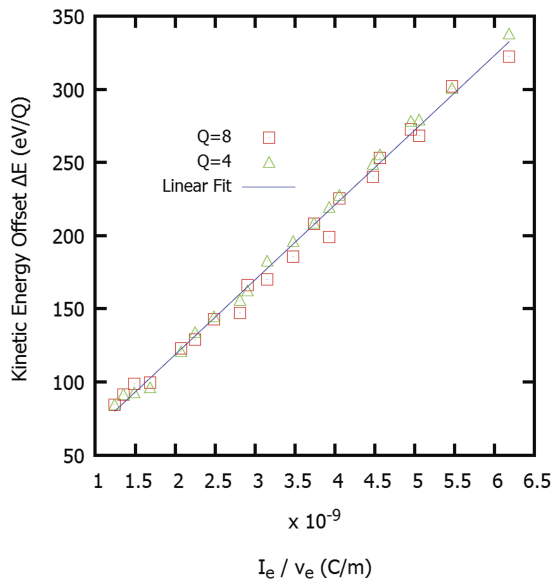


FIG. 5. Measured ΔE values versus the ratio of the electron beam parameters with the EBIS-SC source for both Ar^{3+} (\square) and Ar^{4+} (\triangle) ions. A slope of 5.1×10^{10} Vm/C and an intercept of 16 V is obtained from the shown linear fit and can be used to extract the average electron beam radius ($200 \mu\text{m}$) inside the ion trap (see text).

In Fig. 5, we plot our measured ΔE values versus the ratio of the electron beam parameters that determine the space charge effect (I_e and v_e). As the figure shows, there is a linear relationship between ΔE and this ratio, as expected. This plot can serve as a guide for any measurements which need to account for this offset in the kinetic energy of the MCIs extracted from our EBIS. In addition, the slope “s” of the fit line can be used to determine the radius of the electron beam within the trap region using the equation $r_{\text{electron beam}} = r_{\text{drift tube}} / \exp(0.5(s \times 4\pi\epsilon_0 - 1))$. In this case, we find that our effective electron beam radius is $200 \mu\text{m}$. This value is somewhat larger than quoted elsewhere for similar EBIS designs ($100 \mu\text{m}$).¹⁶ Nevertheless, for in-trap studies of ion-electron interactions typical of EBIS and EBIT machines, the ability to determine the electron beam radius in this way without internally probing the source itself should prove useful.

IV. SUMMARY

We have measured the offset in the kinetic energy of ions extracted from an EBIS source using a downstream RFA. The dependence of the offsets on the electron beam parameters

(current and energy) of the source is in good agreement with an expected variation due to the space charge trapping potential of the electron beam. As the measured beam energies differ by up to a few hundred eV/Q, knowledge of the origin of the offsets and how they can be controlled is important for experiments that seek to use slow MCIs. The linear dependence of the kinetic energy offset on space charge parameters can also be used to extract the radius of the electron beam itself, which can be an important parameter for modeling measurements that focus on the electron-ion interactions within the trap. The measured offsets were attributed solely to the space charge effect of the electron beam without modeling any other in-trap processes.

ACKNOWLEDGMENTS

The authors gratefully acknowledge financial support from the National Science Foundation (No. NSF-DMR-0960100), the Clemson University College of Engineering, Computing and Applied Sciences, and the Clemson University College of Science.

- ¹J. D. Gillaspay, *J. Phys. B: At., Mol. Opt. Phys.* **34**, R93 (2001).
- ²A. Arnaud, F. Aumayr, P. Echenique, M. Grether, W. Heiland, J. Limburg, R. Morgenstern, P. Roncin, S. Schippers, R. Schuch, N. Stolterfoht, P. Varga, T. Zouros, and H. Winter, *Surf. Sci. Rep.* **27**, 113 (1997).
- ³T. Schenkel, A. Hamza, A. Barnes, and D. Schneider, *Prog. Surf. Sci.* **61**, 23 (1999).
- ⁴F. Aumayr and H. Winter, *e-J. Surf. Sci. Nanotechnol.* **1**, 171 (2003).
- ⁵T. Schenkel, A. Persaud, A. Kraemer, J. W. McDonald, J. P. Holder, A. V. Hamza, and D. H. Schneider, *Rev. Sci. Instrum.* **73**, 663 (2002).
- ⁶H. Kurz, F. Aumayr, H. Winter, D. Schneider, M. A. Briere, and J. W. McDonald, *Phys. Rev. A* **49**, 4693 (1994).
- ⁷E. D. Donets, *Rev. Sci. Instrum.* **69**, 614 (1998).
- ⁸M. A. Levine, R. E. Marrs, J. R. Henderson, D. A. Knapp, and M. B. Schneider, *Phys. Scr.* **T22**, 157 (1988).
- ⁹R. Shyam, D. D. Kulkarni, D. A. Field, E. S. Srinadhu, D. B. Cutshall, W. R. Harrell, J. E. Harriss, and C. E. Sosolik, *AIP Conf. Proc.* **1640**, 129 (2015).
- ¹⁰G. Zschornack, V. P. Ovsyannikov, F. Grossmann, A. Schwan, and F. Ullmann, *J. Instrum.* **5**, C08012 (2010).
- ¹¹W. Zhang, K. Yao, Y. Yang, C. Chen, R. Hutton, and Y. Zou, *Phys. Rev. A* **82**, 020702 (2010).
- ¹²R. W. Schmieder, C. L. Bisson, S. Haney, N. Toly, A. R. Van Hook, and J. Weeks, *Rev. Sci. Instrum.* **61**, 259 (1990).
- ¹³R. Becker, M. Kleinod, and H. Klein, *Nucl. Instrum. Methods Phys. Res., Sect. B* **24/25**(Part 2), 838 (1987).
- ¹⁴D. Manura and D. Dahl, SIMION 8.0 User Manual, 2008.
- ¹⁵C. L. Enloe, W. E. Amatucci, M. G. McHarg, and R. L. Balthazor, *Rev. Sci. Instrum.* **86**, 093302 (2015).
- ¹⁶A. Thorn, E. Ritter, A. Sokolov, G. Vorobjev, L. Bischoff, F. Herfurth, O. Kester, W. Pilz, D. B. Thorn, F. Ullmann, and G. Zschornack, *J. Instrum.* **5**, C09006 (2010).